



Thermal cloaking of complex objects with the neutral inclusion and the coordinate transformation methods

Cite as: AIP Advances 9, 045029 (2019); <https://doi.org/10.1063/1.5092128>

Submitted: 07 February 2019 . Accepted: 10 April 2019 . Published Online: 25 April 2019

Qingxiang Ji , Xueyan Chen, Guodong Fang, Jun Liang, Xiangqiao Yan, Vincent Laude , and Muamer Kadic



View Online



Export Citation



CrossMark

AVS Quantum Science

Co-published with AIP Publishing



Coming Soon!



Thermal cloaking of complex objects with the neutral inclusion and the coordinate transformation methods

Cite as: AIP Advances 9, 045029 (2019); doi: 10.1063/1.5092128

Submitted: 7 February 2019 • Accepted: 10 April 2019 •

Published Online: 25 April 2019



Qingxiang Ji,^{1,2}  Xueyan Chen,^{1,2} Guodong Fang,¹ Jun Liang,^{1,3,a)} Xiangqiao Yan,¹ Vincent Laude,²  and Muamer Kadic²

AFFILIATIONS

¹National Key Laboratory of Science and Technology on Advanced Composites in Special Environments, Harbin Institute of Technology, Xidazhi Street, Harbin 150001, China

²Institut FEMTO-ST, CNRS, Université de Bourgogne Franche-Comté, 25000 Besançon, France

³Institute of Advanced Structure Technology, Beijing Institute of Technology, No.5 South Zhongguancun Street, Haidian District, Beijing 100081, China

^{a)}Electronic address: liangjun@bit.edu.cn

ABSTRACT

We explore the cloaking of a complex shape by either the neutral inclusion or the transformation thermodynamics (TT) methods. Thin cloaks are built and the heat cloaking efficiency is investigated for both the steady-state and the transient regimes. We show that the neutral inclusion cloak is more efficient in both regimes, though it has the drawback that the thermal conductivity of the cloaked shape must be known. In practice, the neutral inclusion method is more flexible and easier to implement than the coordinate transformation method, especially for complex shapes.

© 2019 Author(s). All article content, except where otherwise noted, is licensed under a Creative Commons Attribution (CC BY) license (<http://creativecommons.org/licenses/by/4.0/>). <https://doi.org/10.1063/1.5092128>

The idea of an invisibility cloak was first introduced^{1,2} using the transformation optics (TO) approach in the field of electromagnetic waves, based on pioneering works by Dolin³ and Bérenger.⁴ TO was soon extended to many other fields, such as elastic waves,^{5–9} acoustics,^{10–13} and matter waves.^{14–16}

Later, based on the diffusion equation, cloaking of heat flows in thermodynamics was demonstrated.^{17–19} Guenneau¹⁷ firstly built a mathematically covariant formulation of the heat equation for thermal cloaking and concentrating, which opened up possibilities to control heat flows in a manner similar to waves in optics. After some controversy this problem was hopefully closed in 2018.^{20,21} Guenneau and Puvirajesinghe^{22,23} further extended this concept to mass transport using Fick's law.

Recently, Schittny et al.¹⁹ used this method to construct cloaking devices but quickly realized that an alternative method called neutral inclusion (NI) was also available. The NI approach was first derived by Kerner²⁴ in 1956 for the static diffusion equation. Much

work was done since then on both methods, but without a quantitative difference analysis in the case of complex shapes.^{25–31} In fact, the TT approach can in principle always be applied whereas the neutral inclusion is only possible for a set of geometries.^{32,33} It further requires knowledge of the conductivity to be cloaked.

In this paper we implement both methods in the case of a complex shape and evaluate cloaking in both the static and the dynamic regimes. We emphasize a specific geometry with an extremely thin cloaking device. We demonstrate how efficient the NI approach can be, even in the dynamic regime and especially for thin cloaks, when compared to transformation thermodynamics. Besides, we illustrate the deterioration of cloaking as a function of time.

We start by recalling the heat conduction equation in the absence of body heat sources

$$\nabla \cdot (\sigma \nabla T) + \rho c \frac{\partial T}{\partial t} = 0 \quad (1)$$

where σ is the thermal conductivity and T represents the temperature. The heat conduction equation is form invariant when the transformed parameters are given by

$$\sigma = \frac{J \sigma' J^T}{\det(J)}, \quad \rho c = \frac{\rho' c'}{\det(J)} \quad \text{and} \quad J_{xx'} = \frac{\partial(x, y, z)}{\partial(x', y', z')}. \quad (2)$$

In Eq. (2), J is the Jacobian transformation matrix which characterizes the geometrical transformation between the original (virtual) space and the transformed (physical) space. We consider a linear transformation that compresses virtual space ($0 < r' < R_2$) into physical space ($R_1 < r < R_2$) as

$$r = \frac{R_2 - R_1}{R_2} r' + R_1, \quad \theta = \theta', \quad z = z' \quad (3)$$

in cylindrical coordinates and as

$$r = \frac{R_2 - R_1}{R_2} r' + R_1, \quad \theta = \theta', \quad \varphi = \varphi' \quad (4)$$

in spherical coordinates. In the above equations R_1 and R_2 are the inner radius and the outer radius of the cloak, respectively. In the case of cylindrical coordinates, following Eqs. (1–2), using mathematical identities^{34,35} on composed Jacobians ($J_{xx'} = J_{xr} J_{r\theta'} J_{\theta'z'}$) with $J_{xr} = \partial(x, y, z)/\partial(r, \theta, z)$, $J_{r\theta'} = \partial(r, \theta, z)/\partial(r', \theta', z')$ and $J_{\theta'z'} = \partial(r', \theta', z')/\partial(x', y', z')$ we can recognize that $J_{xr} = R(\theta) \text{diag}[1, r, 1]$ where $R(\theta)$ is a rotation matrix leads to $J = R(\theta) \text{diag}[\alpha, r/r', 1] R(-\theta)$ with $\alpha = 1 - R_1/R_2$. Finally, we can get the transformed thermal conductivity in physical space as

$$\frac{\sigma_c}{\sigma_b} = R(\theta) \text{diag}\left[\frac{\alpha r'}{r}, \frac{r}{\alpha r'}, \frac{r'}{\alpha r}\right] R(-\theta) \quad (5)$$

where σ_b is the thermal conductivity of the isotropic background material. For a spherical cloak, the same procedure leads to^{34,35}

$$\frac{\sigma_s}{\sigma_b} = R(\theta, \varphi) \text{diag}\left[\frac{1}{\alpha} \left(\frac{r'}{r}\right)^2, \frac{1}{\alpha}, \frac{1}{\alpha}\right] R(-\theta, -\varphi). \quad (6)$$

In the neutral inclusion method, according to Kerner's analytical results,²⁴ the effective conductivity of an assemblage can be obtained by

$$\sigma_*^c = \sigma_2^c + \frac{2(1-f^c)\sigma_2^c(\sigma_1 - \sigma_2^c)}{2\sigma_2^c + f^c(\sigma_1 - \sigma_2^c)} \quad (7)$$

for a coated cylinder and

$$\sigma_*^s = \sigma_2^s + \frac{3(1-f^s)\sigma_2^s(\sigma_1 - \sigma_2^s)}{3\sigma_2^s + f^s(\sigma_1 - \sigma_2^s)} \quad (8)$$

for a coated sphere, respectively. σ_1 is the thermal conductivity of the inner object and σ_2^c (σ_2^s , respectively) is the conductivity of the layer coating the cylinder (the sphere, resp.). In Eqs. (7–8), $f^c = (1 - R_1^2/R_2^2)$ and $f^s = (1 - R_1^3/R_2^3)$ denote the volume fractions occupied by the coating layer in the assemblage.

We built the object ‘‘HIT’’ which is made up of cylinders and spheres (see Fig. 1). Both the coordinate transformation and the neutral inclusion methods are implemented to cloak this object. For both methods, we built a thin cloaking shell with uniform thickness $a = 0.0187$ m. The geometry parameters are $R_1 = 1$ m and

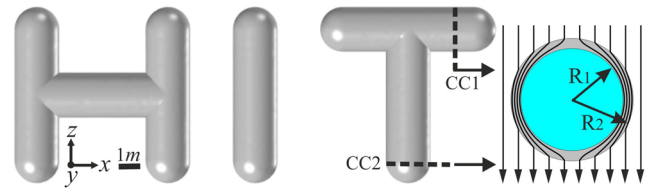


FIG. 1. Geometry definition of the object and of the cloak. On the right-hand side we depict the heat flow lines (when the heat flux is imposed in the y -direction) obtained in the case of cloaking using transformation thermodynamics through the two sections CC1 and CC2.

$R_2 = 1.0187$ m, and the height of the cylinders is $h = 6$ m. The thermal conductivity of the object and of the background are $\sigma_1 = 13.5$ W/(mK) and $\sigma_b = 1$ W/(mK), respectively. Following Eqs. (5–6), we set the transformed thermal conductivity of the coating shell as

$$\sigma_c = \text{diag}\left[\frac{r-1}{r}, \frac{r}{r-1}, \frac{2967.6(r-1)}{r}\right]$$

for cylinders and

$$\sigma_s = 54.48 \text{ diag}\left[\left(\frac{r-1}{r}\right)^2, 1, 1\right]$$

for spheres. Imposing the neutral inclusion conditions $\sigma_*^c = \sigma_*^s = \sigma_b$, results in $\sigma_2^c = 0.02$ W/mK and $\sigma_2^s = 0.02021$ W/mK.

For all cases, finite element simulations based on the commercial software COMSOL Multiphysics are conducted. In the stationary regime, we impose a temperature difference of 1 K between left and right boundaries in the y -direction. Other boundaries are defined as adiabatic boundaries to ensure that conduction is the dominant mode of heat transfer, rather than convection. We plot in Fig. 2 the temperature difference $\Delta T = (T_i - T_r)$, where T_i and T_r are the temperatures of external fields for cloaks ($i = O$ for the obstacle case, $i = NI$ for the NI cloak case, and $i = TT$ for the TT cloak case) and a bare plate ($r = \text{reference case}$). In the obstacle case, the object simply has no coating layer. We can observe in Fig. 2(a) that the obstacle without a cloak leads to significant perturbations to the external temperature field distribution. In contrast, the temperature difference is near-zero throughout the whole probe domain in the NI cloak case (Fig. 2(b)), which demonstrates that the neutral inclusion method is efficient for steady-state cloaking. However, there exist some perturbations in the external temperature field in the TT cloak case (Fig. 2(c)), indicating that thermal cloaking achieved by transformation thermodynamics approach is not perfect. It is seen that perturbations mainly arise near the domain interfaces between cylinders. To eliminate perturbations, a complicated coordinated transformation would be needed, which is beyond the scope of this paper. We note that such a transformation would need to be continuous at the domain interface.

In order to compare quantitatively the TT and the NI cloak, we define an index that characterizes the heat cloaking efficiency as

$$M_V = \frac{\int_{\Omega} |\Delta T| d\Omega}{\int_{\Omega} d\Omega}, \quad (9)$$

where Ω denotes the probe domain of external fields. M_V reveals all perturbations to the external heat profile. Obviously, a lower

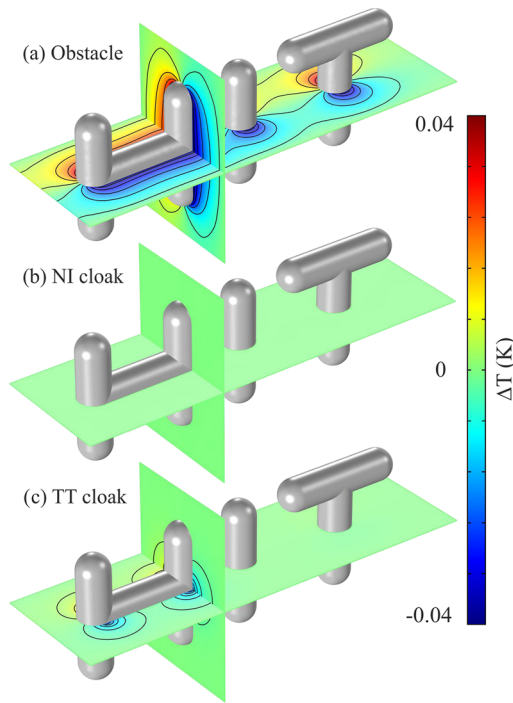


FIG. 2. Steady-state numerical simulation of temperature difference ΔT for (a) the obstacle, (b) the NI cloak, and (c) the TT cloak. Black lines are iso-thermal lines.

value for M_V corresponds to better cloaking. Ideal cloaking would be achieved for $M_V = 0$. We calculated the index for the different cases shown in Table I. Compared to the obstacle case, the neutral inclusion cloak reduces heat perturbations by 2090 times whereas the TT cloak reduces it by 14 times. In the steady-state regime, the neutral inclusion cloak thus shows much higher cloaking efficiency than the TT cloak.

We also implemented transient heat transfer simulations for both the TT approach and the NI method. In the dynamic simulations, we applied a temperature source with a maximum of 1 K on the left side of the domain and attached a perfectly matched layer on its right side. Ambient temperature was fixed to be 0 K. We extract temperature differences ΔT at the cut plane ($x = 6$ m) of both cloaks and plot the results in Fig. 3. For comparison, the results for the obstacle are also presented. It is observed that the external heat profile is strongly disturbed by the obstacle. Distortions are dramatically reduced when the object is coated with the NI cloak, demonstrating that the neutral inclusion method remains efficient even in the dynamic regime. Furthermore, though the TT cloak significantly reduces heat disturbances compared to the obstacle case, perturbations remain significant especially near domain interfaces. Hence,

TABLE I. Calculated heat cloaking efficiency index in the steady-state case.

Geometry	Obstacle	NI cloak	TT cloak
M_V (mK)	16.865	0.008	1.151

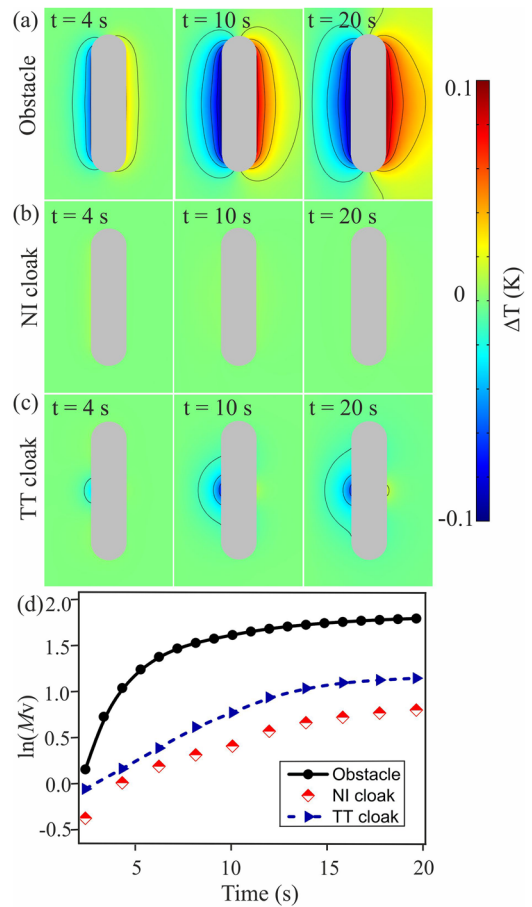


FIG. 3. Dynamic cloaking as a function of time for (a) the obstacle, (b) the NI cloak, and (c) the TT cloak. (d) Quantitative comparison of cloaking for the NI and the TT methods versus time.

the NI cloak performs better for heat cloaking than the TT cloak, even though the design procedure is not fully accurate and domain discontinuities remain. We further calculated the heat cloaking efficiency index in the dynamic regime. It is observed in Fig. 3d that heat perturbations are obviously larger than those of the steady-state case, which demonstrates that thermal cloaking deteriorates if the dynamical part of the heat conduction equation is significant. As the NI cloak does not rely on a transformation technique, it avoids some problems present in TT cloaks, such as extreme thermal conductivity (inhomogeneous, anisotropic, or even singular). Besides, the NI cloak achieves nearly perfect cloaking by regular isotropic materials, which is of interest for real applications.

So far, we have considered with index M_V a quantity integrated over the whole probe domain. We now investigate further the details of the temperature distribution near the object interface, where the external heat profile is most strongly disturbed. We define measurement lines and record temperatures T_i on these lines. Measurement lines are indicated by the red dotted line in Fig. 4, and L_i and L'_i denote measurement lines for the NI cloak and TT cloak, respectively. A heat distribution index is defined as

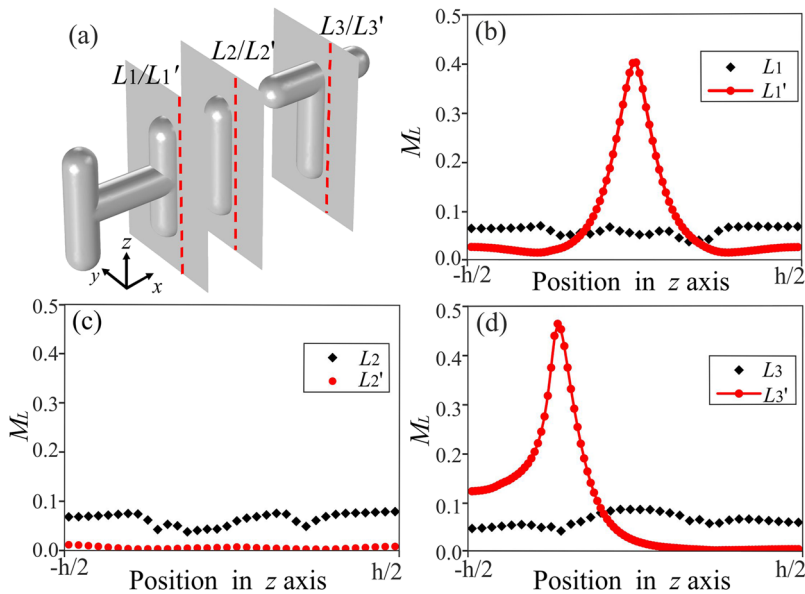


FIG. 4. Temperature perturbation index M_L along measurement lines for the NI and the TT cloaks. (a) Location of measurement lines. (b) M_L along lines L_1 (NI) and L_1' (TT). (c) M_L along lines L_2 (NI) and L_2' (TT). (d) M_L along lines L_3 (NI) and L_3' (TT).

$$M_L = \frac{|T_i - T_r|}{|T_o - T_r|}, \quad (10)$$

where T_r and T_o are the temperatures recorded along measurement lines for the bare plate and for the obstacle, respectively. For the cloak we use the index i for the temperature and the lines are depicted in the Fig. 4. The larger the value of M_L , the larger the temperature perturbations and thus the worse the cloaking. We calculate the distribution index for both methods and plot the results in Fig. 4. We observe that the distribution index values recorded at points near the interface of the object are significantly larger for the TT cloak than those for the NI cloak. In other regions, smaller values and thus better cloaking performances are observed for the TT cloak. Complicated coordinate transformations would be needed to improve the TT cloak, but that would bring in more difficulties in design and fabrication.

In summary, we have implemented both the neutral inclusion method and the transformation optics approach to cloak thermally a complex shape including cylinders and spheres. The neutral inclusion cloak appears more efficient in both steady-state and transient regimes. The TT cloak indeed presents some perturbations near the interface with the object; they are the main reason leading to imperfect cloaking. Besides, we have shown that cloaking deteriorates when temporal aspects become significant. Finally, the neutral inclusion method appears more practicable in view of potential applications, especially for complex shapes for which the conductivity of the object is known.

This work was supported by the National Natural Science Foundation of China (11732002 and 11672089). Qingxiang Ji acknowledges support by China Scholarship Council. Muamer Kadic acknowledges support by the EIPHI Graduate School (contract "ANR-17-EURE-0002") and by the French Investissements d'Avenir program, project ISITEBFC (contract "ANR-15-IDEX-03").

REFERENCES

- J. B. Pendry, D. Schurig, and D. R. Smith, *Science* **312**, 1780 (2006).
- U. Leonhardt, *Science* **312**, 1777 (2006).
- L. S. Dolin, *Izv. Vuz. Radiofiz.* **4**, 964 (1961).
- J.-P. Berenger, *Journal of Computational Physics* **114**, 185 (1994).
- G. W. Milton, M. Briane, and J. R. Willis, *New J. Phys.* **8**, 248 (2006).
- A. Diatta and S. Guenneau **49**, 445101 (2016).
- M. Farhat, S. Guenneau, and S. Enoch, *Phys. Rev. Lett.* **103**, 024301 (2009).
- M. Brun, S. Guenneau, and A. B. Movchan, *Appl. Phys. Lett.* **94**, 061903 (2009).
- N. Stenger, M. Wilhelm, and M. Wegener, *Phys. Rev. Lett.* **108**, 014301 (2012).
- M. Farhat, S. Guenneau, S. Enoch, A. Movchan, F. Zolla, and A. Nicolet, *New Journal of Physics* **10**, 115030 (2008).
- R. V. Craster and S. Guenneau, *Acoustic metamaterials: Negative refraction, imaging, lensing and cloaking*, vol. 166 of Springer Series in Materials Science (Springer Science & Business Media, 2012), ISBN 9789400748132.
- S. A. Cummer and D. Schurig, *New Journal of Physics* **9**, 45 (2007).
- M. Farhat, S. Enoch, S. Guenneau, and A. B. Movchan, *Phys. Rev. Lett.* **101**, 134501 (2008).
- S. Zhang, D. A. Genov, C. Sun, and X. Zhang, *Phys. Rev. Lett.* **100**, 123002 (2008).
- A. Greenleaf, Y. Kurylev, M. Lassas, and G. Uhlmann, *New Journal of Physics* **10**, 115024 (2008).
- M. McCall, J. B. Pendry, V. Galdi, Y. Lai, S. Horsley, J. Li, J. Zhu, R. C. Mitchell-Thomas, O. Quevedo-Teruel, P. Tassin *et al.*, *Journal of Optics* **20**, 063001 (2018).
- S. Guenneau, C. Amra, and D. Veynante, *Opt. Express* **20**, 8207 (2012).
- S. Guenneau and T. M. Puvirajesinghe, *J. Roy. Soc. Inter.* **10**, 20130106 (2013).
- R. Schittny, M. Kadic, S. Guenneau, and M. Wegener, *Phys. Rev. Lett.* **110**, 195901 (2013).
- R. Craster, S. Guenneau, H. Hutridurga, and G. Pavliotis, *Multiscale Modeling & Simulation* **16**, 1146 (2018).
- D. Petiteau, S. Guenneau, M. Bellieud, M. Zerrad, and C. Amra, *Scientific Reports* **4**, 7386 (2014).
- S. Guenneau and T. Puvirajesinghe, *Journal of the Royal Society Interface* **10**, 20130106 (2013).
- T. M. Puvirajesinghe, Z. Zhi, R. Craster, and S. Guenneau, *Journal of the Royal Society Interface* **15**, 20170949 (2018).

- ²⁴E. H. Kerner, *Proc. Phys. Soc. B* **69**, 808 (1956).
- ²⁵D. Bigoni, S. Serkov, M. Valentini, and A. Movchan, *International Journal of Solids and Structures* **35**, 3239 (1998).
- ²⁶S. Mannherz, A. Niemeyer, F. Mayer, C. Kern, and M. Wegener, *Opt. Express* **26**, 34274 (2018).
- ²⁷M. Farhat, P.-Y. Chen, H. Bagci, C. Amra, S. Guenneau, and A. Alù, *Scientific Reports* **5**, 9876 (2015).
- ²⁸K. P. Vemuri and P. R. Bandaru, *Applied Physics Letters* **103**, 133111 (2013).
- ²⁹T. Han, X. Bai, D. Gao, J. T. Thong, B. Li, and C.-W. Qiu, *Physical Review Letters* **112**, 054302 (2014).
- ³⁰X. He and L. Wu, *Physical Review E* **88**, 033201 (2013).
- ³¹S. Narayana and Y. Sato, *Phys. Rev. Lett.* **108**, 214303 (2012).
- ³²G. W. Milton, *The Theory of Composites* (Cambridge University Press, 2002).
- ³³G. W. Milton and S. K. Serkov **457**, 1973 (2001).
- ³⁴F. Zolla, S. Guenneau, A. Nicolet, and J. B. Pendry, *Opt. Lett.* **32**, 1069 (2007).
- ³⁵A. Nicolet, F. Zolla, Y. Ould Agha, and S. Guenneau, *COMPEL* **27**, 806 (2008).